Materials Science and Engineering A355 (2003) 216–230

MATERIALS SCIENCE & ENGINEERING A

www.elsevier.com/locate/msea

On the influence of mechanical surface treatments—deep rolling and laser shock peening—on the fatigue behavior of Ti–6Al–4V at ambient and elevated temperatures

R.K. Nalla [a], I. Altenberger [b], U. Noster [b], G.Y. Liu [a], B. Scholtes [b], R.O. Ritchie [a,*]

[a] Department of Materials Science and Engineering, University of California, Berkeley, CA 94720-1760, USA
[b] Institute of Materials Engineering, University Kassel, Kassel, Germany

Received 28 October 2002; received in revised form 16 January 2003

Abstract

It is well known that mechanical surface treatments, such as deep rolling, shot peening and laser shock peening, can significantly improve the fatigue behavior of highly-stressed metallic components. Deep rolling (DR) is particularly attractive since it is possible to generate, near the surface, deep compressive residual stresses and work hardened layers while retaining a relatively smooth surface finish. In the present investigation, the effect of DR on the low-cycle fatigue (LCF) and high-cycle fatigue (HCF) behavior of a Ti–6Al–4V alloy is examined, with particular emphasis on the thermal and mechanical stability of the residual stress states and the near-surface microstructures. Preliminary results on laser shock peened Ti–6Al–4V are also presented for comparison. Particular emphasis is devoted to the question of whether such surface treatments are effective for improving the fatigue properties at elevated temperatures up to ~450 °C, i.e. at a homologous temperature of $\sim 0.4T/T_m$ (where T_m is the melting temperature). Based on cyclic deformation and stress/life (S/N) fatigue behavior, together with the X-ray diffraction and in situ transmission electron microscopy (TEM) observations of the microstructure, it was found that deep rolling can be quite effective in retarding the initiation and initial propagation of fatigue cracks in Ti–6Al–4V at such higher temperatures, despite the almost complete relaxation of the near-surface residual stresses. In the absence of such stresses, it is shown that the near-surface microstructures, which in Ti–6Al–4V consist of a layer of work hardened nanoscale grains, play a critical role in the enhancement of fatigue life by mechanical surface treatment.

Keywords: Fatigue; Surface treatment; Residual stress; Deep rolling; Laser shock peening; Ti–6Al–4V; Elevated temperature behavior

1. Introduction

The control of failures due to high-cycle fatigue (HCF) in turbine engine components is one of the most critical challenges currently facing the US Air Force [1–3]. In general, components such as blades and disks are subjected to HCF loading associated with the high frequency (1–2 kHz) vibrations within the engine, superimposed on to a low-cycle fatigue (LCF) component associated with the start and stop cycles. In order to increase the resistance of such components to the initiation and early growth of fatigue cracks under such conditions, especially in the presence of foreign-object damage, mechanical surface treatments are widely used. Such treatments, such as deep rolling, shot peening and laser shock peening, are known to significantly improve resistance to wear and stress corrosion, and in particular to enhance the fatigue strength of highly-stressed metallic components used in a variety of engineering applications [4–6].

Though shot peening has traditionally been used for most aircraft components, deep rolling (DR) offers several attractive advantages due to the generation of

* Corresponding author. Tel.: +1-510-486-5798; fax: +1-510-486-4881.
E-mail address: roritchie@lbl.gov (R.O. Ritchie).

0921-5093/03/$ - see front matter
doi:10.1016/S0921-5093(03)00069-8

a deeper 'case' of compressive residual stresses[1] and a work hardened microstructure as well as a relatively smoother surface finish [7]. The process involves plastic deformation of the near-surface layers of the metallic work-piece by a spherical or cylindrical rolling element under a controlled force or pressure. In contrast to roller burnishing, which is performed with lower pressures and solely serves to achieve a smooth surface topography, the aim of this treatment is to induce deep compressive residual stresses and work hardened surface layers.

Although deep rolling is restricted to certain component geometries, the process is relatively inexpensive and has the advantage that the lower surface roughness levels achieved act to lower the chance of fatigue crack initiation whereas the compressive residual stresses act to retard subsequent crack propagation [8–10]. For this reason, deep rolling is increasingly utilized to enhance the fatigue strength and service lives of steel components, such as crankshafts [11], especially in the presence of detrimental notches.

In the present work, we examine the effectiveness of deep rolling for improving the fatigue behavior of a commonly-used turbine-engine alloy, Ti–6Al–4V, with special emphasis on the near-surface residual stress states and microstructures, before and after mechanical and/or thermal exposure. Results are compared with those obtained using laser shock peening (LSP), where a short, high-power laser pulse is used (under a water blanket) to vaporize a sacrificial coating on the component, thereby producing a shock wave that propagates inwards from the surface (see [12] for details). Akin to DR, LSP offers many advantages compared to shot peening in that the process is capable of introducing deep cases of compressive residual stresses and cold work in the near-surface layers without compromising the surface roughness (which remains relatively unaffected by LSP). Moreover, this process is not restricted by component geometry, as is the case with deep rolling.

The observed improvement in the fatigue lifetime due to mechanical surface treatments is known to depend predominantly on the amount, depth distribution and stability of the induced residual stresses and work hardening in the near-surface regions [13]. Consequently, but for a few exceptions [14,15], elevated service temperatures are generally believed to be detrimental to the fatigue response of surface treated components, owing to the partial (or, in some cases, total) relaxation of the induced residual stress state. In fact, there is a paucity of results in archival literature dealing with the effectiveness of such mechanical surface treatments at temperatures above ambient [16–18]. For this reason, an objective of this work is to investigate the effectiveness of mechanical surface treatments at increasing temperature. Specifically, the cyclic fatigue performance of Ti–6Al–4V is evaluated, before and after DR and LSP, at both ambient and elevated temperatures up to 450 °C, i.e. between ~ 0.15 and $0.4T/T_m$, where T_m is the melting temperature. Results are discussed in the context of the stability of the residual stresses and near-surface microstructure with increasing temperature.

2. Experimental procedures

2.1. Materials

The Ti–6Al–4V alloy used in the present study originated as double vacuum-arc remelted forging stock, produced by Teledyne Titanium (Pittsburgh, PA) specifically for the US Air Force-sponsored joint government-industry-academia High-Cycle Fatigue Program. The chemical composition of this alloy (in wt.%) is given in Table 1 [19].

The original, 63.5 mm diameter bar-stock was sectioned into 400 mm long sections, preheated to 940 °C for 30 min and forged as glass-lubricant coated bars at this temperature into $400 \times 150 \times 20$ mm plates [19]. These plates were subsequently solution-treated for 1 h at 925 °C, fan-air cooled and then stress relieved for 2 h at 700 °C. The resulting microstructure, termed bimodal or solution treated and overaged (STOA), consisted of a distribution of interconnected equiaxed primary-α grains (64% by volume) and lamellar α+β colonies (transformed-β) (Fig. 1). The average α-grain size was ~ 20 μm, with slight elongation in the longitudinal (L) direction of the forging; the average α-lath spacing was 1–2 μm. Using differential thermal analysis, the β-transus temperature was measured to be 990–1005 °C.

Uniaxial tensile tests were conducted in the L-orientation using a constant strain rate of 5×10^{-4} s^{-1}. In addition, plane-strain fracture toughness tests were performed using fatigue-precracked 25 mm thick compact-tension specimens machined in the L-T orientation. Room temperature results, in terms of the measured yield and tensile strengths, ductility and toughness, are listed in Table 2, together with additional data from [19]. The corresponding yield strengths at 250 and 450 °C were, respectively, 675 and 575 MPa [23].

2.2. Mechanical surface treatments

Unnotched, cylindrical specimens with a gauge length of 15 mm and diameter of 7 mm were used for the surface treatment and subsequent fatigue studies. After machining, the specimens were stress relieved in vacuo for 2 h at 700 °C to minimize any residual machining stresses. For deep rolling, a standard spherical rolling

[1] Typical case depths for shot peening are less than 300 μm for soft metals, such as aluminium alloys and mild steels, and are significantly shallower for harder materials.

Table 1
Chemical composition of Ti–6Al–4V bar stock (wt.%) [19]

Bar location	Ti	Al	V	Fe	O	N	H
Top	Bal.	6.27	4.19	0.20	0.18	0.012	0.0041
Bottom	Bal.	6.32	4.15	0.18	0.19	0.014	0.0041

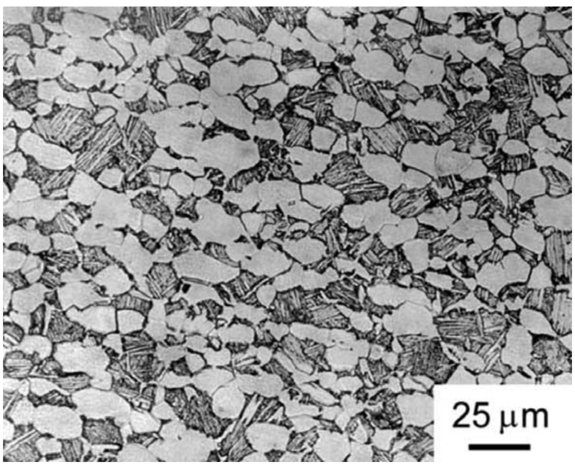

Fig. 1. Optical micrograph of the bimodal (solution treated and overaged, STOA) Ti–6Al–4V microstructure investigated in the present study. Etched for ~10 s in five parts 70% HNO_3, ten parts 50% HF, 85 parts of H_2O. Average grain size is about 20 μm, with slight grain elongation in the L-direction.

element (6.6 mm diameter) was used with a constant feed of 0.1125 mm per revolution and a rolling pressure of 150 bar (rolling force ~500 N), yielding a ‘coverage’ of 1000%. Laser shock peening was carried out with a power density of 7 GW cm^{-2} using two overlapping layers of shocks (coverage of 200%). The shocks were applied simultaneously to both sides of the part (to maintain straightness) using 2.6 × 2.6 mm beams in 18 ns pulses yielding a fluence (power density) of 7 GW cm^{-2}. Surface roughness was measured using a mechanical sensor (‘Perthometer’ by Mahr Company, Göttingen, Germany) for the untreated state and for both the surface treated states to obtain the average roughness depth, R_z, which is a 10-point average distance between the five highest peaks and five highest valleys within the sampling length from the roughness profile. Additionally, the microhardness of the near-surface regions was measured on carefully mechanically polished cross-sections for all three states investigated (virgin, DR and LSP) using a standard Vickers indenter with an indentation load of 0.1 kg.

2.3. S/N fatigue testing and cyclic deformation behavior

Tension-compression ‘smooth-bar’ stress/life (*S*/*N*) fatigue tests were performed under load control using a standard servo-hydraulic testing machine operating at a frequency of 5 Hz (sine wave). Both ‘virgin’ and surface treated (DR) specimens were tested at 25 °C ($T/T_m = 0.15$) and 450 °C ($T/T_m = 0.4$); limited additional testing was performed on LSP samples at 450 °C and on DR and LSP samples at 250 °C ($T/T_m \sim 0.3$). Alternating stresses, σ_a, between 450–750 and 350–550 MPa, were used at 25 and 450 °C, respectively, at a constant load ratio (minimum load/maximum load) of $R = -1$, i.e. with a zero mean stress (σ_m), and the cycles to failure N_f measured. For the tests at 250 and 450 °C, specimens were heated with a small thermostatically controlled furnace. Once the required temperature was reached (generally within ~45 min), specimens were held for a further 45 min before starting the actual test. During fatigue cycling, the axial strain was monitored using a capacitative extensometer (Eichhorn and Hausmann Company, Karlsruhe, Germany).

Cyclic deformation behavior was evaluated by registering the full hysteresis loops during the fatigue tests at pre-defined numbers of cycles, using a strain extensometer with a resolution of 0.001%. The plastic strain amplitudes were measured from the half widths of the hysteresis loops (Fig. 2a).

2.4. Residual stress determination

Residual stress distributions were obtained by applying standard X-ray diffraction techniques using line shifts of X-ray diffraction peaks [20]. Lattice strain measurements were carried out using Cr–K_α radiation at the {201}-planes of the hexagonal α-phase. For residual stress evaluation, the $\sin^2\psi$-method was ap-

Table 2
Uniaxial tensile and toughness properties of Ti–6Al–4V at 25 °C

Yield strength (σ_y) (MPa)	Ultimate tensile strength (MPa)	Reduction in area (%)	Fracture toughness K_{Ic} (MPa$\sqrt{m}$)
930	978	45	64

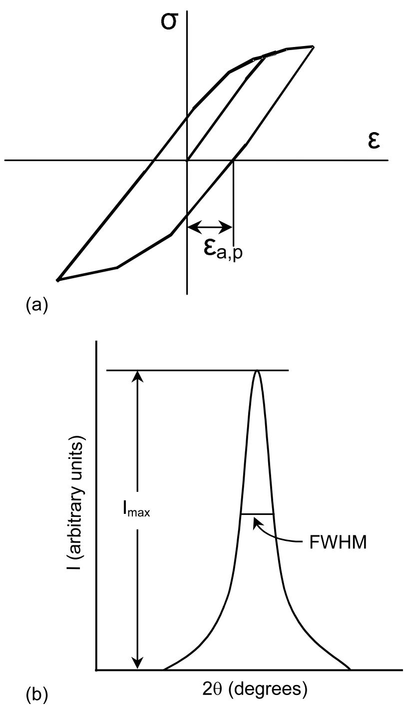

Fig. 2. Schematic illustrations of the definition of (a) the plastic strain amplitude, $\sigma_{a,p}$ measured during fatigue testing, and (b) the full width at half maximum (FWHM) for the X-ray diffraction measurements.

plied using the elastic constant $1/2s_2 = (1+\nu)/E = 12.09 \times 10^{-6}$ mm^2 N^{-1}; details of this technique are provided elsewhere [21]. Residual stress depth profiles were determined (without correction for stress relief) by successive removal of material electrochemically in steps of 20–50 μm. Near-surface work hardening was characterized by hardness measurements as well as by the full width at half maximum (FWHM) distributions (shown schematically in Fig. 2b) of the X-ray interference lines. It is well known that FWHM values are a useful means to characterize the degree of work hardening present, since they usually correlate well with the hardness in soft and medium-hard mechanically surface treated materials [9]. Measurements were made on the hourglass samples in the virgin (untreated) state and following surface treatment, in the following conditions:

- after mechanical surface treatment (DR and LSP states),
- after thermal annealing (for 45 min at 450 °C) (virgin, DR and LSP states),
- after fatigue cycling at 25 °C to half the cycles to failure, $N_f/2$ ($\sigma_a = 670$ MPa, $R = -1$, 5 Hz) (virgin, DR and LSP states),
- after fatigue cycling at 250 °C to half the cycles to failure, $N_f/2$ ($\sigma_a = 550$ MPa, $R = -1$, 5 Hz) (DR state), and
- after fatigue cycling at 450 °C to half the cycles to failure, $N_f/2$ ($\sigma_a = 460$ MPa, $R = -1$, 5 Hz) (virgin, DR and LSP states).

2.5. Electron microscopy characterization

Transmission electron microscopy (TEM) was carried out using a 200 kV JEOL microscope on cross-sections cut perpendicular to the surface of the deep rolled specimens; details of the TEM-preparation methods are given elsewhere [22]. Additionally, the effect of temperature was investigated by heating one such specimen in situ in the TEM from room temperature up to 900 °C ($T/T_m \sim 0.6$). The in situ TEM was performed at the National Center for Electron Microscopy (Berkeley, CA) using a JEOL 3010 300 kV TEM, equipped with a Gatan 652 double tilt heating holder and a Gatan 794 Slow Scan CCD for imaging purpose. The sample holder temperatures were calibrated in a separate vacuum system to ensure accuracy to ±20 °C. The bright field images taken were from sample areas that were relatively thick so as to alleviate concerns with respect to sample surfaces altering the grain growth behavior.

Fractographic observations were performed using standard scanning electron microscopy (SEM) operating in the secondary electron mode. In particular, the spacing of the fatigue striations on the fracture surfaces was measured on surfaces perpendicular to the incoming electron beam. Five readings, each at five different locations equidistant from the crack initiation site at the surface, were taken and the average computed. These measurements were intended to give an indication of the local fatigue crack-growth rate per cycle.

3. Results

3.1. Fatigue properties

3.1.1. S/N behavior

A comparison of the stress/life (S/N) fatigue behavior (at $R = -1$) of the virgin and the deep rolled Ti–6Al–4V at temperatures of 25 and 450 °C is shown in Fig. 3. It can be seen that deep rolling leads to a significant enhancement in the observed fatigue lifetime at room temperature, particularly in the high-cycle fatigue regime; indeed at $\sigma_a = 500$ MPa, lives are increased by roughly two orders of magnitude. However, this beneficial influence of deep rolling is still apparent, although reduced, at 450 °C; specifically, lives are increased in the HCF regime by roughly one order of magnitude at $\sigma_a = 400$ MPa. For both virgin and DR conditions, fatigue lives were considerably lower at 450 °C than at 25 °C, presumably due to the lower yield strength at the higher temperature.

Although the largest effect of the mechanical surface treatment is seen in the HCF regime, the effect is also significant in the low-cycle regime. This is shown in Fig. 4 where the LCF lifetimes of virgin and DR samples are

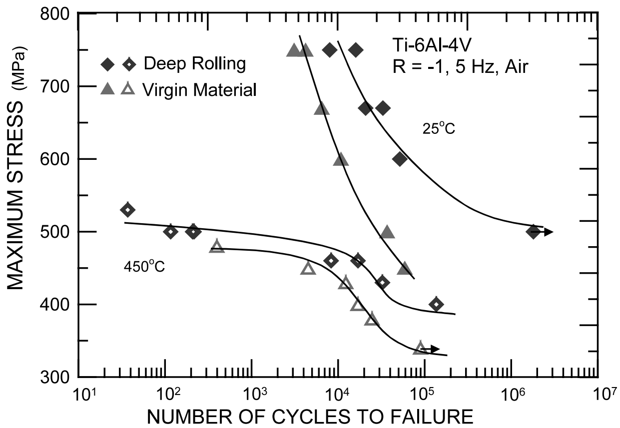

Fig. 3. Stress/life (S/N) data obtained at 25 and 450 °C for the virgin and deep rolled Ti–6Al–4V material. A beneficial effect of deep rolling can be seen, even at elevated temperature.

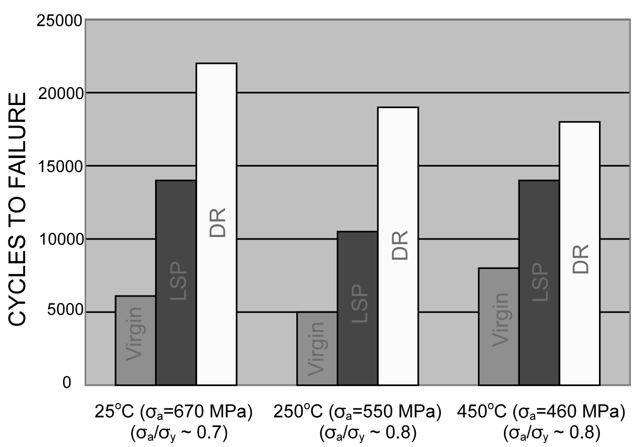

Fig. 4. Enhancement in fatigue lifetimes following deep rolling and laser shock peening for test temperatures of 25, 250 and 450 °C and stress amplitudes of 670, 550 and 460 MPa, respectively. The lifetime improvement induced by deep rolling can be seen to be superior to that induced by laser shock peening.

compared at 25 and 450 °C at applied stress amplitudes close to the yield strength, respectively, at 670 and 460 MPa, ($\sigma_a/\sigma_y \sim 0.7$–$0.8$). Also shown for comparison are the equivalent fatigue lifetimes after laser shock peening. Similar to previous studies [12,24,25], both mechanical surface treatments can be seen to confer significant improvements in the fatigue lives, even in the LCF regime. In the present work, it is apparent that the DR process is considerably more effective than LSP for the process parameters investigated. Moreover, it is clear that this beneficial effect of both DR and LSP processes persists in Ti–6Al–4V at temperatures as high as 43% of the melting temperature.

Similar to the results at 450 °C, limited fatigue tests at 250 °C ($\sigma_a = 550$ MPa, $\sigma_a/\sigma_y \sim 0.8$) also showed longer fatigue lifetimes for the surface treated conditions as compared with the virgin material (Fig. 4); in addition, for the processing conditions utilized, DR was again more effective than LSP in enhancing the fatigue life.

3.1.2. Crack-growth rates

Whereas the presence of the mechanical treated surface is generally considered to enhance S/N fatigue lifetimes primarily by inhibiting the initiation of cracks, SEM measurements of the spacings of the fatigue striations on the fracture surfaces also show a beneficial effect in slowing down the initial crack-propagation rates. Fig. 5 shows SEM images of the striations and the local crack-growth rates estimated from their spacings on the fracture surfaces of virgin and deep rolled Ti–6Al–4V cycled at 25 and 450 °C at stress amplitudes of, respectively, 750 and 400 MPa[2]. These results indicate that deep rolling has an additional positive influence on fatigue properties by lowering the initial fatigue-crack growth rates, typically by a factor of 2–3, compared with corresponding behavior in the virgin material. Again, it is important to note that this beneficial effect of the mechanical surface treatment is not restricted solely to ambient temperatures, but it is also clearly in evidence at 450 °C.

3.1.3. Plastic strain amplitude

The plastic strain amplitude, measured during S/N tests, can be considered as a reliable measure of the extent of 'damage' during the fatigue of ductile materials [27]. In Fig. 6a, the plastic strain amplitude, is shown so monitored, as a function of the number of the applied cycles during fatigue testing of the virgin, DR and LSP conditions at 450 °C (at $\sigma_a = 460$ MPa, $R = -1$). For all three material conditions, an initial increase (cyclic softening) and subsequent decrease (cyclic hardening) in the plastic strain amplitude was observed. Compared with the virgin material, deep rolling was observed to lower the plastic strain amplitude throughout the majority of the lifetime; for a given applied stress, such a reduced plastic strain amplitude would be expected to result in a significantly extended lifetime, as observed experimentally. This effect was also apparent for the LSP condition, although its magnitude was somewhat reduced. Fig. 6a also shows that there is an initial quasi-elastic 'incubation' period prior to cyclic softening in the untreated material; this incubation phase is absent for DR samples, where cyclic softening is seen from the very first cycle. The reason for this difference in behavior is believed to be the significantly higher dislocation density in the work hardened surface layers in the case of deep rolling [28]. At room

[2] For this range of fatigue-crack growth rates, i.e. between $\sim 10^{-6}$ and 10^{-5} m per cycle, the fatigue striation spacings in Ti–6Al–4V alloys, are reasonably representative of the macroscopic growth rates [26].

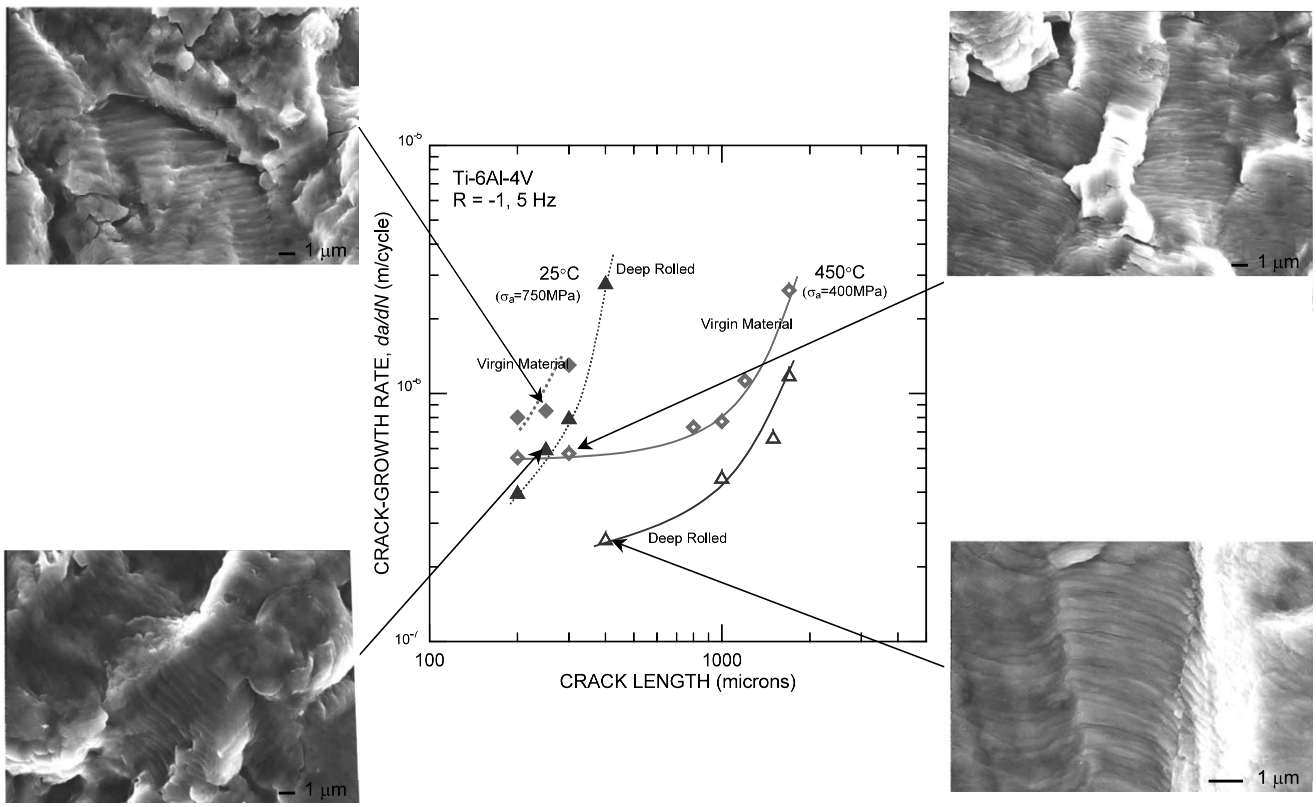

Fig. 5. Local fatigue-crack growth rates at 25 and 450 °C, estimated from striation spacing measurements on fracture surfaces of untreated and deep rolled Ti–6Al–4V. Deep rolling can be seen to result in lower initial fatigue-crack growth rates at both temperatures.

temperature (at $\sigma_a = 670$ MPa, $R = -1$), the virgin and LSP samples showed no measurable plastic strain amplitudes, i.e. the amplitudes were less than the 0.001% resolution of the extensometer used, while the DR samples showed similar behavior, except very close to the actual fracture event (strain amplitudes of 0.01% were measured). Similar measurements were also performed at 250 °C ($\sigma_a = 550$ MPa, $R = -1$), and are shown in Fig. 6b. At this temperature, the virgin material exhibited cyclic softening throughout the entire lifetime, whereas both the surface treated conditions initially cyclically softened before subsequently cyclically hardening until fracture.

3.2. *Surface roughness and hardness*

Surface roughness measurements were made before and after mechanical surface treatments. While laser shock peening did not result in any significant alteration of the surface topography, deep rolling led to a marked decrease (by more than 50%) in the measured roughness depth, R_z. Specifically, compared with a surface roughness of $R_z = 1.7$ µm in the virgin material, the surface roughness depth of the deep rolled samples was $R_z = 0.8$ µm. This is in contrast to shot peening which generally increases the roughness of conventionally ground, turned or polished surfaces [29]. Such smoother surfaces associated with deep rolling can lead to significant improvements in resistance to fatigue-crack initiation and hence contribute to the beneficial effect that this surface treatment can have in prolonging fatigue lifetimes.

Hardness profiles, taken perpendicular to the surface of the virgin, DR and LSP microstructures, revealed the existence of a work hardened layer in the surface treated samples. Fig. 7 shows the near-surface hardness depth profiles for all conditions; compared with a Vickers hardness of ~330 VPN in the virgin material, both DR and LSP structures showed a greater than 10% increase near the surface. 'Case' depths for the work hardened material were ~500–1000 µm. Compared with the microstructure of the virgin material, TEM of the surface-treated structures revealed significantly higher dislocation densities, estimated to be on the order of 10^{11} cm^{-2}, in the near-surface layers (Fig. 8), consistent with the increase in hardness there.

3.3. *Residual stresses and work hardening induced by surface treatment*

To evaluate the magnitude of the residual stress states and the extent of work hardening induced in the near-surface layers by the mechanical surface treatments, X-ray diffraction measurements were performed on the

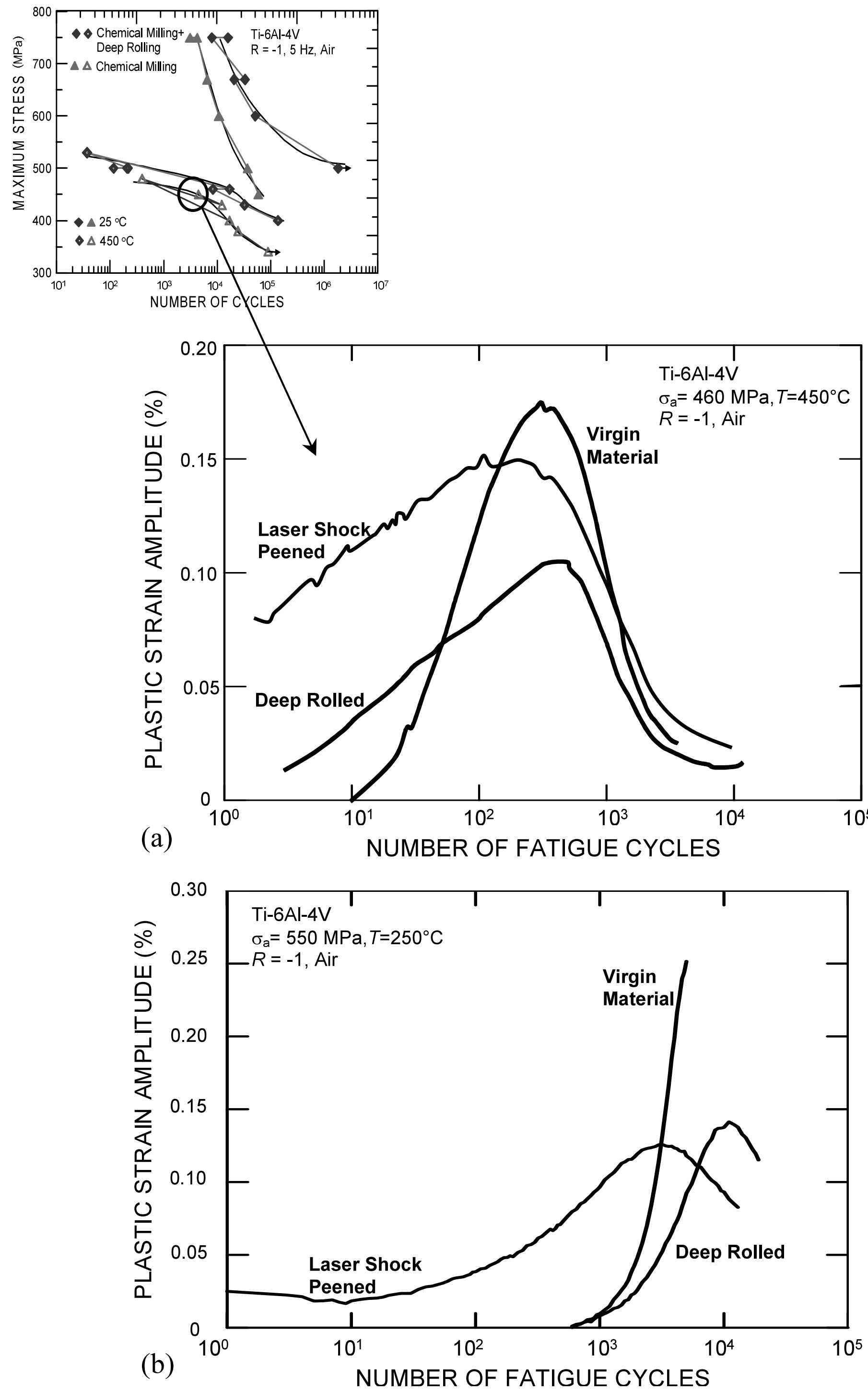

Fig. 6. (a) Plastic strain amplitudes for the virgin, deep rolled and laser shock peened Ti–6Al–4V measured during high temperature fatigue cycling at 450 °C ($\sigma_a = 460$ MPa, $R = -1$, 5 Hz) and (b) 250 °C ($\sigma_a = 550$ MPa, $R = -1$, 5 Hz), as a function of the number of applied cycles. Note the reduction in the strain amplitude levels due to mechanical surface treatment.

virgin and surface treated (DR and LSP) specimens prior to fatigue cycling. It was observed that both mechanical surface treatments introduced significant levels of compressive residual stresses at the specimen surface and in the near-surface regions. Fig. 9 shows the profiles of the residual stresses, together with line

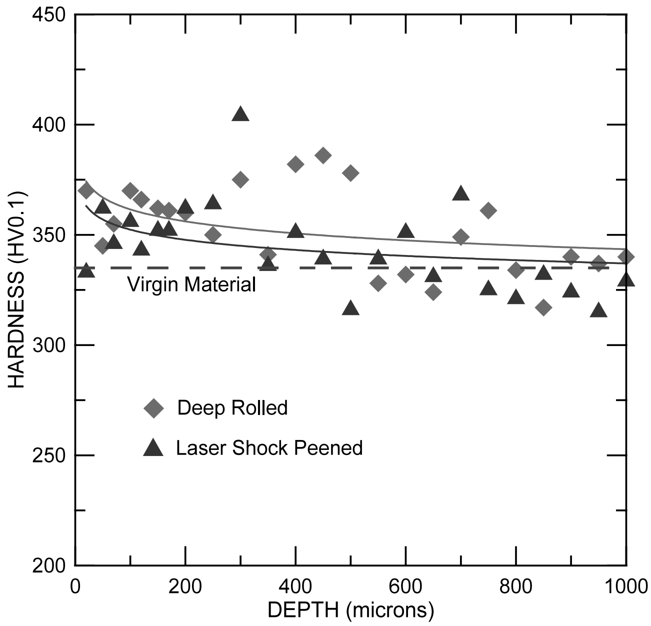

Fig. 7. Near-surface hardness depth profile of deep rolled and laser shock peened Ti–6Al–4V. The hardness level for the virgin material (330 VPN) is shown for comparison.

broadening measurements of the 'half-widths' (full width at half maximum, FWHM-see Fig. 2b), as a function of depth into the surface. It is apparent that after deep rolling, maximum compressive residual stresses as high as 930 MPa, i.e. comparable with the UTS in compression, are evident immediately below the surface (Fig. 9a); these compressive stresses decay to baseline (virgin material) levels over a depth of approximately 500 μm. Average compressive residual stress levels were considerably lower in the LSP material, with a maximum value just below the surface of ~450 MPa; however, the residual stress 'case' was deeper than that produced by DR and more uniform in magnitude. Similar observations of a deep residual stress 'case' following LSP have been reported previously for this material [31].

The corresponding depth profiles of the variation in the half-width (FWHM) values, which are a measure of the degree of work hardening [9,10], are shown in Fig. 9b. It is clear that the DR material shows significantly higher near-surface work hardening than the LSP material, with a sharper decay to the virgin material levels. Indeed, similar to the residual stress profiles, these measurements indicate a DR 'case' depth of roughly 500 μm. In general, the residual stress levels and the degree of near-surface work hardening are less pronounced after LSP, although the extent of the 'case' does appear to be deeper. Such residual stress and FWHM depth profiles after deep rolling correspond qualitatively to those found after shot peening in Ti–6Al–4V, as described in [32].

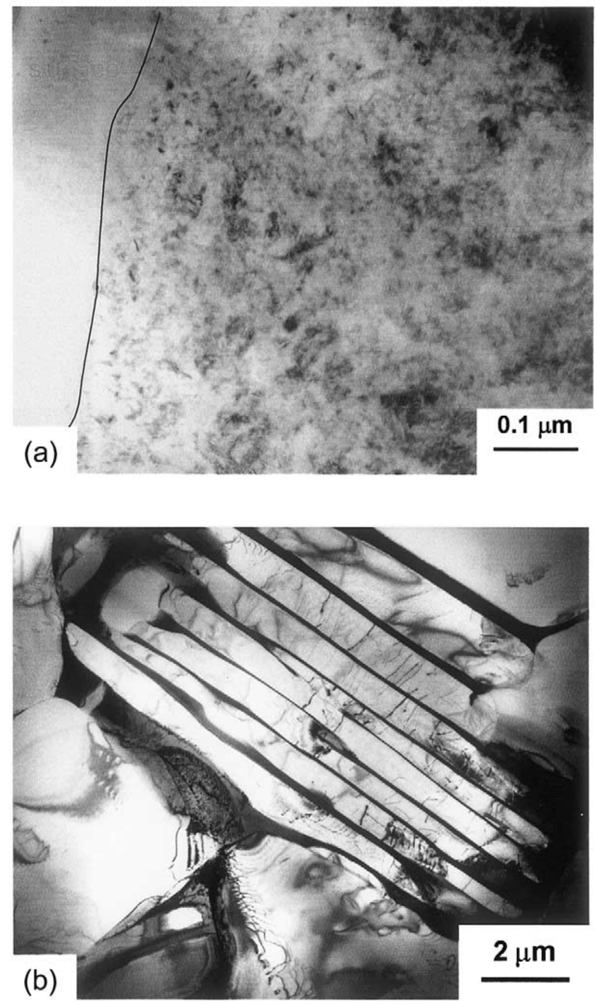

Fig. 8. TEM of (a) near-surface regions of deep rolled Ti–6Al–4V (rolling pressure 150 bar) prior to fatigue cycling, and (b) the virgin material [30], the latter showing globular primary-α phase within a lamellar α+β matrix (alternating α-lamellae: bright contrast; β-lamellae: dark contrast). Note the dislocation tangles and nanoscale sub-grain structures that are evident in the near-surface region of the surface treated material.

TEM characterization of the near-surface microstructure in deep rolled Ti–6Al–4V is shown in Fig. 8a. It can be seen that deep rolling leads to the formation of highly tangled dislocation arrangements; in addition, the first stages of a diffuse sub-grain structure are formed, typical of the early stages of mechanically-induced nanocrystallization resulting from severe plastic deformation [33–35].

3.4. Effect of fatigue cycling at room temperature

Corresponding residual stress and FWHM depth profiles, taken on specimens fatigued to half the lifetime, $N_f/2$ ($\sigma_a = 670$ MPa) at 25 °C, are shown in Figs. 10 and 11 for the deep rolled and laser shock peened structures, respectively. Results for the virgin state (untreated and unfatigued) and unfatigued surface-treated states are

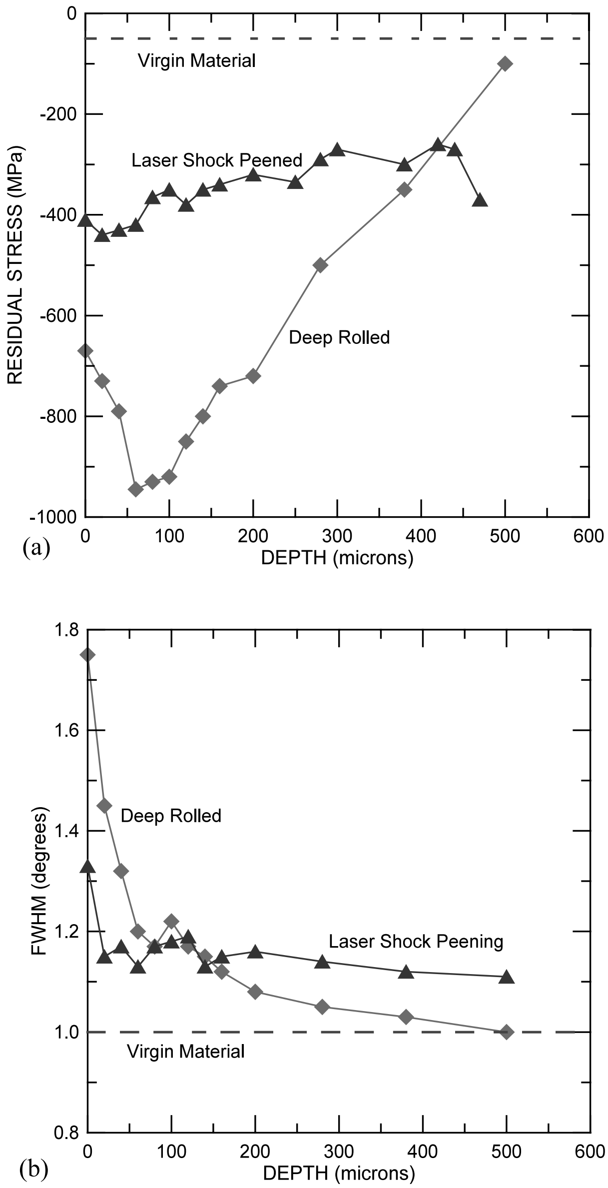

Fig. 9. (a) Near-surface residual stresses and (b) FWHM-values as a function of depth into the surface of deep rolled and laser shock peened Ti–6Al–4V, as compared with the virgin material.

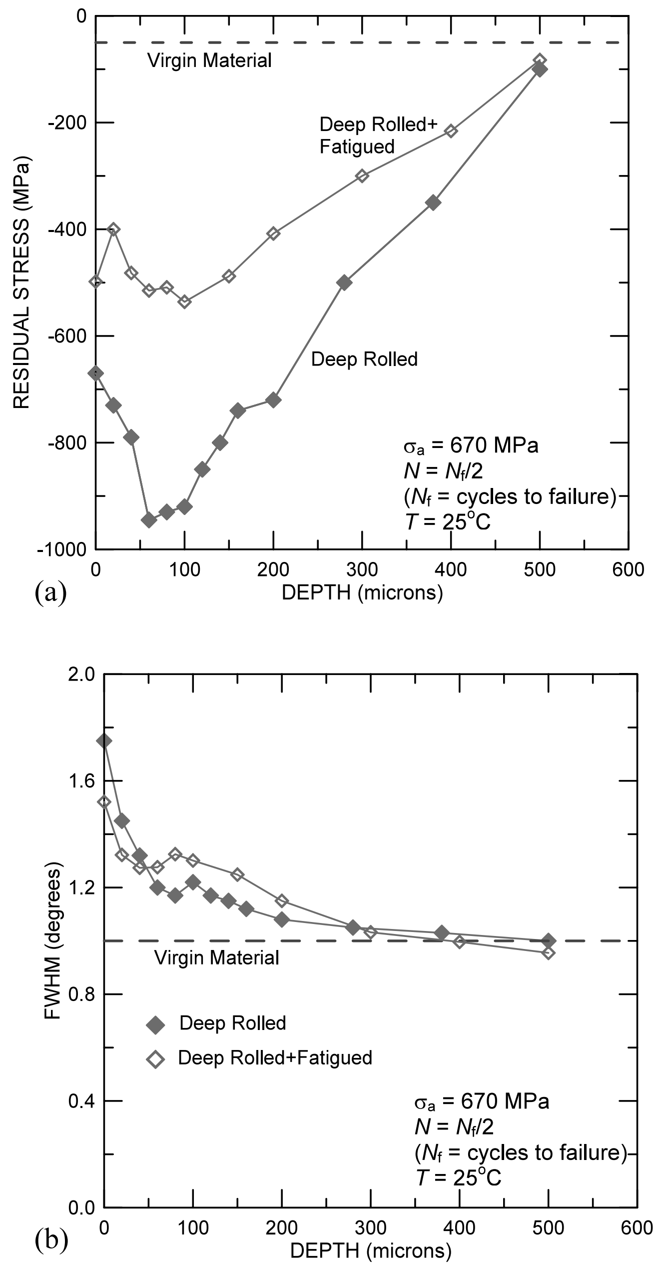

Fig. 10. (a) Residual stress and (b) FWHM profiles as a function of depth into the surface for deep rolled Ti–6Al–4V before and after fatigue cycling at 25 °C. Results for the virgin material are shown for comparison.

also shown for comparison. As noted above, consistent with substantial enhancement in the room-temperature fatigue resistance of Ti–6Al–4V after mechanical surface treatment (Figs. 3 and 4), deep compressive residual stress states exist after both DR and LSP. However, it is apparent that a marked relaxation of these residual stresses occurs on fatigue cycling, especially for deep rolled material (Fig. 10a). Specifically, although a more uniform compressive residual stress remains in place after cycling, the maximum compressive stress level is significantly reduced (by $\sim$30% from the as-DR levels). A similar relaxation occurs on cycling the LSP material, but the reduction in residual stress levels is far less (Fig. 11a).

In contrast, the FWHM distributions for both DR and LSP materials, shown respectively in Fig. 10b and Fig. 11b, are far more stable. These results indicate that the presence of the work hardened layer, and its associated higher dislocation density, appear to be relatively unaffected by the fatigue cycling. As with the surface treated conditions, in general, both the magnitude of the residual stresses and FWHM levels remain more pronounced after cycling for DR material compared with LSP. Such results are consistent with the correspondingly longer lifetimes for the deep rolled specimens (Fig. 4).

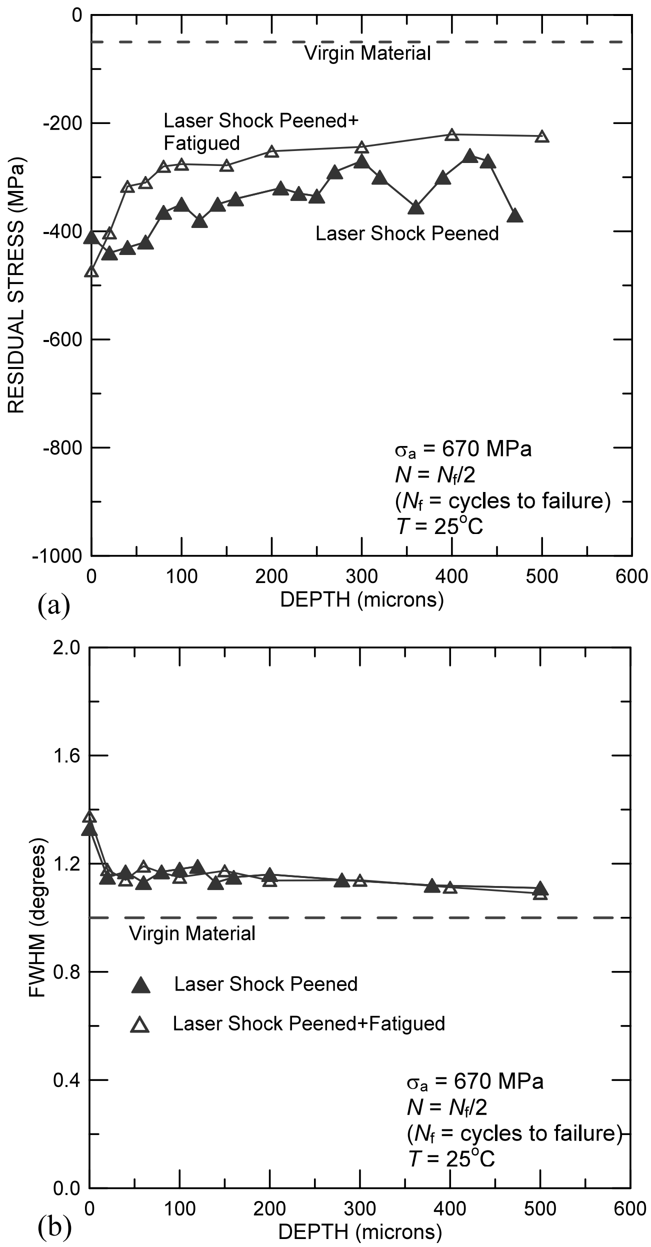

Fig. 11. (a) Residual stress and (b) FWHM profiles as a function of depth into the surface for laser shock peened Ti–6Al–4V before and after fatigue cycling at 25 °C. Results for the virgin material are shown for comparison.

3.5. Effect of temperature

Equivalent results for the residual stress and FWHM profiles at elevated temperatures are presented in Figs. 12–14. Specifically, shown in Figs. 12 and 13 are measurements for the DR and LSP materials, respectively, following fatigue cycling at 450 °C ($\sigma_a = 460$ MPa), again for half the number of cycles to failure, and corresponding measurements following purely thermal exposure at 450 °C, i.e. after simple thermal annealing (with no cycling) for 45 min at 450 °C (roughly corresponding to the duration of the fatigue tests). Also shown for comparison are the residual stress levels and FWHM values for the virgin and as-surface treated conditions.

It can be seen from these results in Fig. 12a and Fig. 13a that whereas thermal exposure alone at 450 °C does cause a substantial reduction in the near-surface compressive residual stresses, fatigue cycling at this temperature causes the almost complete relaxation of the residual stress state in both the DR and LSP conditions. The effect once again is far more pronounced for the DR material, but for both processes the remaining compressive residual stress at the surface was only

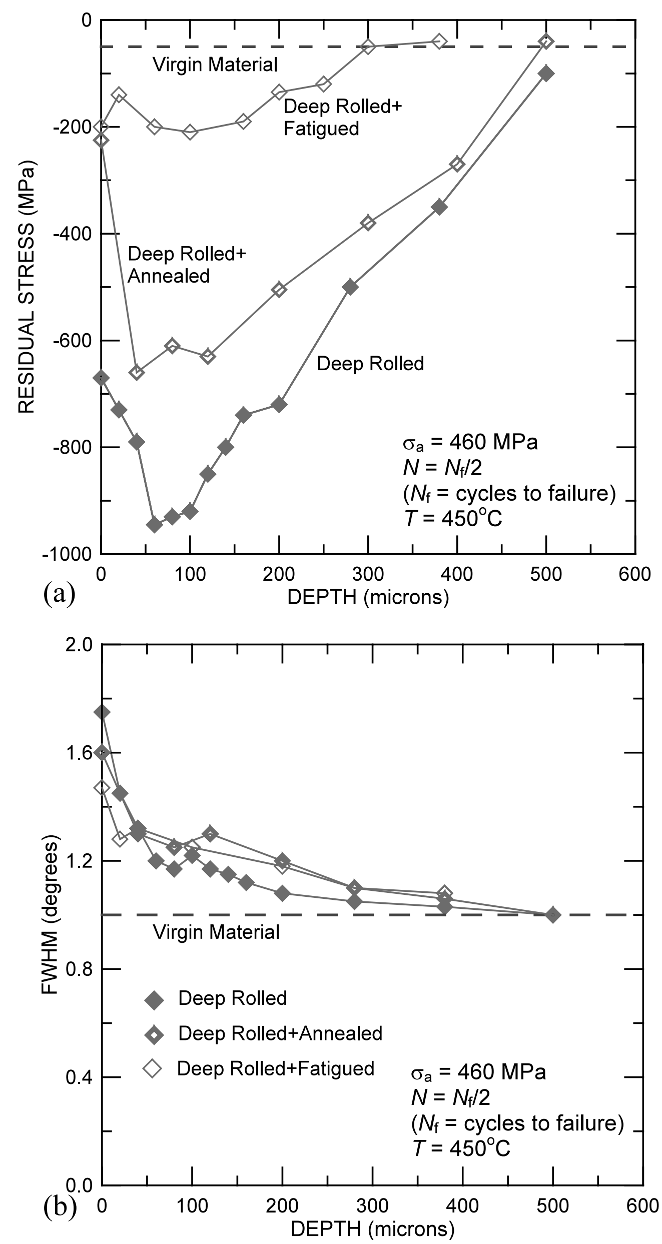

Fig. 12. (a) Residual stress and (b) FWHM profiles as a function of depth into the surface for Ti–6Al–4V in the as deep rolled, deep rolled and 450 °C annealed, and deep rolled and 450 °C fatigued conditions are compared with corresponding results for the virgin material.

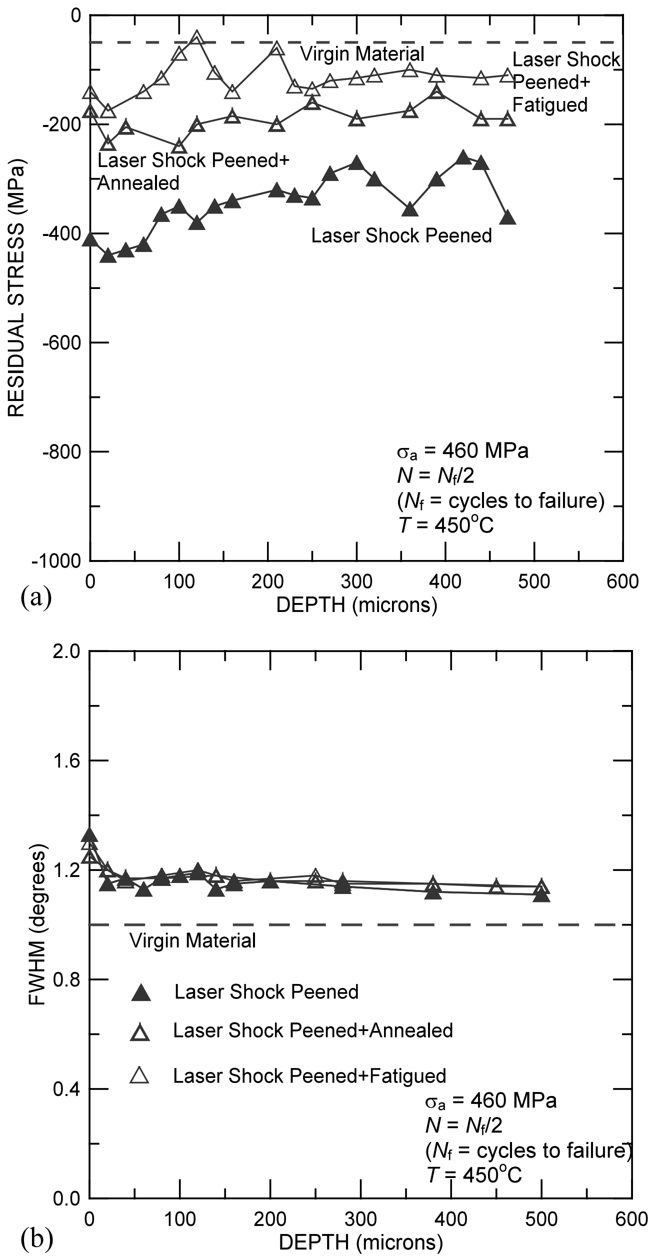

Fig. 13. (a) Residual stress and (b) FWHM profiles as a function of depth into the surface for Ti–6Al–4V in the as laser shock peened (LSP), LSP and 450 °C annealed, and LSP and 450 °C fatigued conditions are compared with corresponding results for the virgin material.

−200 MPa, representing a value 2–3.5 times smaller than the as-surface treated conditions. In comparison, the FWHM values for both DR and LSP material remained essentially unchanged following either 450 °C thermal exposure or fatigue cycling at this temperature. Once again, this implies that the near-surface work hardened layer is quite stable at these temperatures, with or without the presence of cyclic loading.

Since deep rolling and laser shock peening have been shown to still have a beneficial effect on the HCF and LCF properties at this temperature (Figs. 3 and 4), where almost complete relaxation of the residual stress state has occurred, it would appear that the stability of this near-surface work hardened microstructure, and its effect in reducing the cyclic plastic strain (Fig. 5), is the more important factor controlling the enhancement the fatigue lives at 450 °C. The higher near-surface work hardening levels and concomitant superior fatigue lives for the DR, as compared with the LSP, material are consistent with this conclusion.

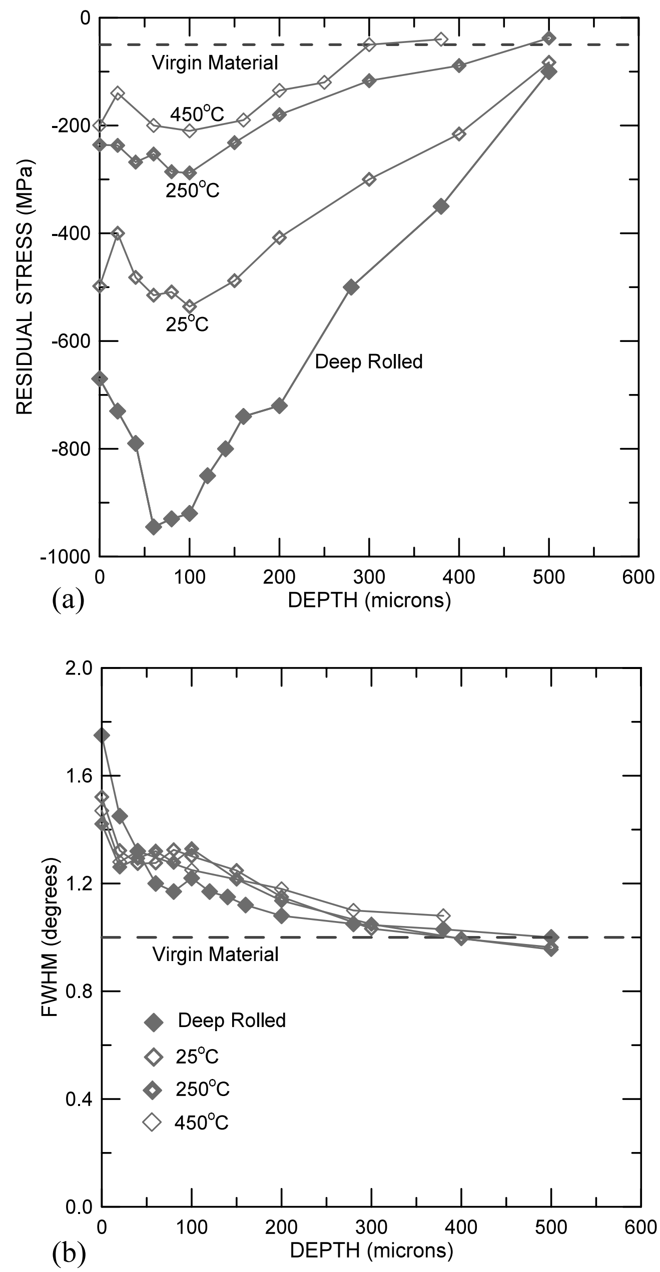

Fig. 14. (a) Residual stress and (b) FWHM profiles as a function of depth into the surface for deep rolled Ti–6Al–4V before and after fatigue cycling at 25, 250 and 450 °C. Results for the virgin material are shown for comparison.

It is interesting to note, however, the extent to which the residual stress state relaxes as a function of the fatigue cycling temperature in surface treated Ti–6Al–4V. In Fig. 14, measurements of the depth profiles of the compressive residual stresses and the FWHM values are plotted for the DR material after fatigue cycling at temperatures between ambient and 450 °C. Whereas the FWHM values and hence the degree of work hardening remain stable to the thermal and mechanical excursions, the compressive stresses in the ~500 μm deep, near-surface case can be seen to progressively degrade with the fatigue cycling temperature. In this regard, behavior at 250 °C, which is more typical of turbine engine environments for most Ti–6Al–4V components, can be seen to be quantitatively very similar to behavior at 450 °C.

3.6. Characterization of the near-surface microstructure

TEM characterization of the work hardened surface layer, shown in Fig. 8a for the deep rolled condition, revealed a heavily dislocated nanoscale microstructure. From the FWHM measurements described above, this structure appears to be quite stable up to 450 °C. Further verification of this was achieved using in situ TEM of DR samples slowly heated from ambient temperature up to 900 °C ($T/T_m \sim 0.6$), with a holding time of 5 min per temperature. Results, presented in Fig. 15, indicate that the surface nanostructure is perfectly stable at 450 °C, and for short durations even up to 900 °C.

4. Discussion

The results of this work clearly indicate the beneficial effect of mechanical surface treatment, specifically by deep rolling and laser shock peening, in enhancing both the ambient-temperature HCF- and LCF resistance of Ti–6Al–4V. The results further show that the effect, which is associated with an increased lifetime and lower initial crack-propagation rates, can be attributed to the creation of a favorable compressive residual stress state within 500–1000 μm of the surface, coupled microstructurally with the formation of a work hardened near-surface layer. Indeed, sub-surface compressive stresses after deep rolling were comparable to the UTS, and roughly half that value following LSP. Such DR and LSP processes overcome some of the disadvantages of the more traditional shot peening process, which has been the most widely used surface treatment procedure for titanium engine components. For example, shot peened alloys may require an additional polishing step to eliminate the induced higher surface roughness, which can lead to a deleterious reduction in the gas flow efficiency of turbine engines. Laser shock peening, conversely, results in little or no increase in surface roughness and deep rolling actually improves it, as described in Section 3.2. Furthermore, both the deep rolling and laser shock peening procedures give rise to deeper case depths, which makes them an attractive option for thin components such as turbine engine compressor blades.

For the process parameters used, deep rolling was found to induce the larger near-surface compressive residual stresses and degree of work hardening as compared with laser shock peening, although the depth of the affected near-surface layer was larger with the latter process. Moreover, DR was observed to markedly reduce the surface roughness. In terms of the resulting improvement in fatigue performance, the deep rolling process was correspondingly found to the confer the larger increases in fatigue lifetimes at a given applied stress for all test temperatures investigated (Fig. 4).

Despite the fact that this improvement in fatigue properties in Ti–6Al–4V from DR and LSP can be ascribed to alterations in the near-surface microstructure and residual stress state (and in the case of DR to reduced surface roughness), a major conclusion from this study is that the beneficial effect in life extension is still evident, although reduced, at temperatures as high as 450 °C (~0.4 T_m) where, due to mechanical cycling and thermal effects, there has been almost complete relaxation of the near-surface compressive residual stresses. Accordingly, it is believed that the benefit of the surface treatments at higher temperatures is associated primarily with the induced work hardened near-surface layer, with its ultrafine grain size and high dislocation density. Such layers are shown to be particularly stable, both mechanically to fatigue cycling at temperatures as high as 450 °C (Fig. 14) and thermally to temperatures excursions as high as 900 °C (Fig. 15). The effect of these hardened layers is to suppress crack initiation and initial crack growth, as observed. However, their overall effect is to reduce the plastic strain amplitude over the majority of the life, as measured experimentally and shown in Fig. 6; since the plastic strain amplitude represents the driving force governing fatigue damage and failure, it is reasoned that this is the primary factor resulting in the lifetime extension at higher temperatures.

Previous studies [36] on shot peening of titanium alloys have indicated a beneficial effect of shot peening at high temperatures but only when subsequent mechanical polishing was carried out. Similar results were found for a shot peened Udimet 720 LI Nickel-base alloy [37] fatigued at elevated temperature. This again clearly indicates the role of near-surface work hardening in fatigue enhancement. Since work hardening primarily retards crack initiation, it is especially effective if the fatigue damage process is crack initiation controlled. Conversely, if mechanically surface treated components

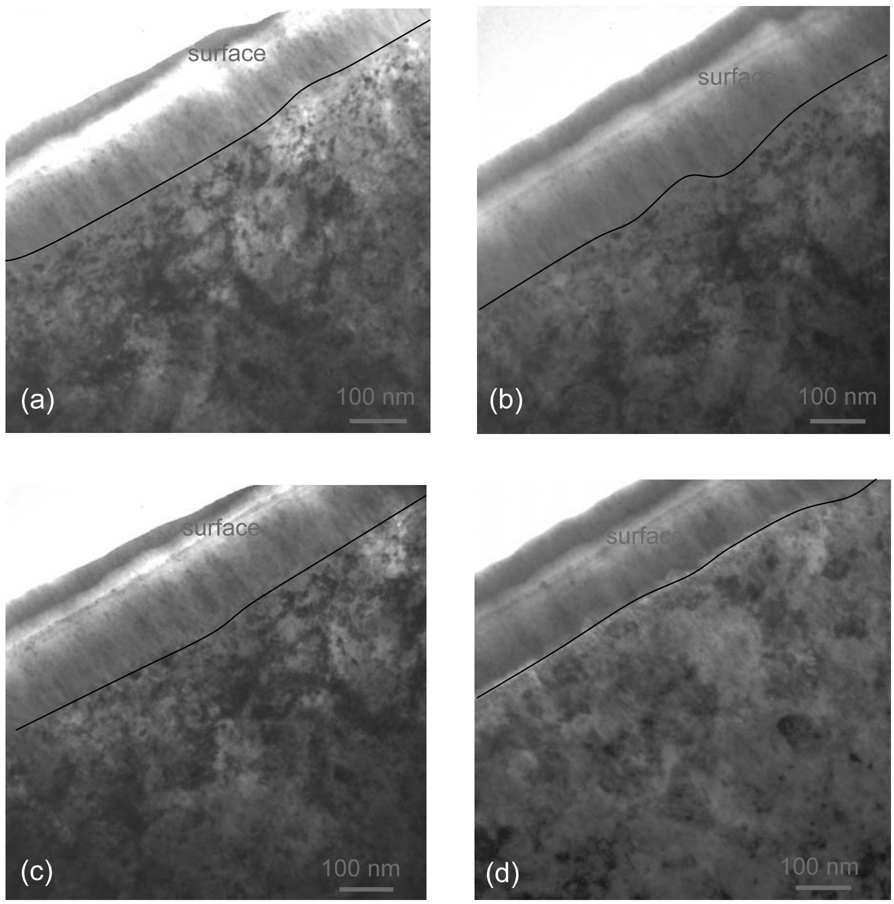

Fig. 15. TEM of deep rolled Ti–6Al–4V during in situ heating to 900 °C, showing the same region of the near-surface microstructure at (a) 25 °C ($T/T_m \sim 0.15$), (b) 250 °C ($T/T_m \sim 0.3$), (c) 450 °C ($T/T_m \sim 0.4$), and (d) 900 °C ($T/T_m \sim 0.6$). The stability of the near-surface structure with increasing temperature is evident.

exhibit very rough surfaces (as for example after conventional shot peening), the fatigue damage process can be considered crack propagation controlled, requiring pronounced and stable compressive residual stresses in order to improve fatigue strength and life significantly. Consequently, the importance of the smoother surfaces of laser shock peened or deep rolled surfaces as compared with conventionally shot peened surfaces cannot be underestimated, especially for high temperature applications. Other studies on high temperature fatigue of shot-peened Ti–6Al–4V alloys [38] have also suggested that the work hardened layers are more stable than the residual stresses at higher temperatures; however, here the beneficial effect on fatigue life was not very pronounced due to the high roughness of the shot peened surfaces.

These observations, along with the current results, clearly imply that for elevated temperature service below $T/T_m \sim 0.4$, the deeper near-surface work hardened layers associated with deep rolling and laser shock peening (with appropriately optimized parameters) provide an excellent means of fatigue life extension for Ti–6Al–4V alloys in the LCF and especially HCF regimes. Moreover, of the two techniques, deep rolling appears to offer the most benefit at higher temperatures (for components where the process can be used) due to higher work hardening and smoother surfaces which act to lessen the probability of crack initiation there.

5. Conclusions

Based on an experimental investigation of the effect of mechanical surface treatments, specifically deep rolling and laser shock peening, on the HCF- and LCF behavior of Ti–6Al–4V at temperatures from ambient up to 450 °C ($T/T_m \sim 0.4$), the following conclusions can be made.

Deep rolling can enhance the HCF and LCF strength of Ti–6Al–4V. While laser shock peening also resulted in an improvement in fatigue strength, deep rolling was found to be more effective for the process parameters investigated.

The beneficial effect on fatigue life at ambient temperatures from the DR and LSP processes can be ascribed to the creation of significant near-surface compressive residual stresses and a near-surface work hardened layer. The greater effectiveness of the deep rolling is attributed to a higher magnitude of induced compressive stresses, a higher degree of work hardening, and the fact that the process results in a significant decrease in the surface roughness.

Based on results at 250 and 450 °C ($T/T_m \sim 0.3$–0.4), both deep rolling and laser shock peening are also found to result in extended fatigue lives at elevated temperatures, although the effect is smaller than at 25 °C.

Although almost complete relaxation of residual stresses occurred at 450 °C, the benefit in high temperature fatigue resistance from the mechanical surface treatment is found to be primarily associated with the formation of a near-surface work hardened layer with a nano-scale microstructure that is stable during thermal exposure or fatigue cycling at temperatures up to and, exceeding, 450 °C. The effect of this work hardened layer is to reduce the plastic strain amplitude, which acts to lessen the driving force for fatigue damage.

Acknowledgements

This work was supported in part by the US Air Force Office of Scientific Research under Grants No. F49620-96-1-0478 (under the auspices of the Multidisciplinary University Research Initiative on High Cycle Fatigue) and No. F49620-02-1-0010 to the University of California at Berkeley. Thanks are also due to Metal Improvement Company, Livermore, CA, for performing the laser shock peening and to DFG (Deutsche Forschungsgemeinschaft) for financial support to Dr. I. Altenberger under Grant No. AL 558/1-1. The authors also wish to thank Dr E.A. Stach of the National Center for Electron Microscopy, Berkeley, CA, for assistance with the in situ transmission electron microscopy.

References

[1] Report of the AdHoc Committee on Air Force Aircraft Jet Engine Manufacturing and Production Processes, United States Air Force Scientific Advisory Board, SAF/AQQS: The Pentagon, Washington, DC, 1992.
[2] J.C.I. Chang, An Integrated Research Approach to Attack Engine HCF Problems, Air Force Office of Scientific Research, Bolling AFB, Washington, DC, 1996.
[3] B.A. Cowles, Int. J. Fract. 80 (1996) 147.
[4] G.S. Was, R.M. Pelloux, Met. Trans. A10 (1979) 656.
[5] E.R. de los Rios, P. Mercier, B.M. El-Sehily, Fatigue Fract. Eng. Mater. Struct. 19 (1996) 175.
[6] I. Altenberger, B. Scholtes, in: K. Kenny, S. Brebbia (Eds.), Surface Treatment IV, WIT press, Southampton, UK, 1999, p. 281.
[7] H. Wohlfahrt, P. Krull (Eds.), Mechanische Oberflächenbehandlungen, Wiley-VCH, Weinheim, 2000.
[8] A. Niku-Lari (Ed.), Advances in Surface Treatments, Pergamon Press, Oxford, 1987.
[9] B. Scholtes, Assessment of residual stresses, in: V. Hauk (Ed.), Structural and Residual Stress Analysis by Nondestructive Methods, Elsevier, Amsterdam, 1997, p. 590.
[10] G.A. Webster, in: H.P. Lieurade (Ed.), Fatigue and Stress of Engineering Materials and Structures, IITT-International, Gournay-Sur-Marne, France, 1989, p. 9.
[11] H. Felgentreu, G. Berstein, Mechanische Oberflächenbehandlung, DGM-Informationsgesellschaft Verlag, Oberursel, 1989, p. 175.
[12] C.S. Montross, T. Wei, L. Ye, G. Clark, Y.W. Mai, Int. J. Fat. 24 (2002) 1021.
[13] I. Altenberger, J. Gibmeier, R. Herzog, U. Noster, B. Scholtes, Mater. Sci. Res. Int. 1 (2001) 275.
[14] M.C. Berger, J.K. Gregory, Mater. Sci. Eng. 263A (1999) 200.
[15] R. Menig, V. Schulze, O. Vöhringer, Z. Metallkunde 93 (2002) 7.
[16] H. Holzapfel, V. Schulze, O. Vöhringer, Mater. Sci. Eng. A248 (1998) 9.
[17] U. Noster, I. Altenberger, B. Scholtes, in: K.U. Kainer (Ed.), Magnesium Alloys and Their Applications, Wiley-VCH, Weinheim, 2000, p. 312.
[18] N. Hasegawa, Y. Watanabe, Y. Kato, in: D. Kirk (Ed.), Proceedings of the Fifth International Conference On Shot Peening, Oxford, UK, 1993, p. 157.
[19] D. Eylon, Summary of Available Information on the Processing of the Ti–6Al–4V HCF/LCF Program Plates, Univ. of Dayton, Report 1998.
[20] B.D. Cullity, Elements of X-ray diffraction, 2nd., Addison-Wesley, Menlo Park, CA, 1978, p. 447.
[21] E. Macherauch, P. Müller, Z. F. Angew. Physik 13 (1961) 305.
[22] U. Martin, I. Altenberger, K. Kremmer, H. Oettel, B. Scholtes, Mater. Sci. Eng. 246A (1998) 69.
[23] Metals Handbook, Properties and Selection, Non-ferrous Alloys and Special-Purpose Materials, vol. 2, 10th ed., ASM International, Materials Park, OH, 1990.
[24] A. Drechsler, T. Dörr, L. Wagner, Mater. Sci. Eng. A 243 (1998) 217.
[25] G. Hammersley, L.A. Hackel, F. Harris, Optics Lasers Eng. 34 (2000) 327.
[26] Y.N. Lenets, R.S. Bellow, Int. J. Fat. 22 (2000) 521.
[27] L.F. Coffin, Trans. ASME 76 (1954) 931.
[28] B. Scholtes, I. Altenberger, U. Noster, in: T. Chandra, K. Higashi, C. Suryanarayana, C. Tome (Eds.), Proceedings of the International Conference on Processing and Manufacturing of Advanced Materials- Thermec 2000 (Special Issue: J. Mater. Processing Tech.), Sec. A1, Vol. 117/3, Elsevier Science, UK, 2001.
[29] B. Scholtes, Eigenspannungen in mechanisch randsschichtverformten werkstoffzuständen, DGM Informationsgesellschaft, Oberursel, Germany, 1990.
[30] J.O. Peters, R.O. Ritchie, Eng. Fract. Mech. 67 (2000) 193.
[31] M.J. Shepard, P.R. Smith, P.S. Prevey, A.H. Clauer, in: A.H. Clauer (Ed.), Proceedings of the Sixth National HCF Conference, Jacksonville, FL, 2001.
[32] L. Wagner, in: R.R. Boyer, D. Eylon, G. Lütjering (Eds.), Fatigue Behavior of Titanium Alloys, The Minerals, Metals & Materials Society, Warrendale, PA, 1999, p. 253.

[33] I. Altenberger, B. Scholtes, U. Martin, H. Oettel, Mater. Sci. Eng. 264A (1999) 1.
[34] K. Lu, J. Lu, J. Mater. Sci. Technol. 15 (1999) 193.
[35] C. Moelle, Ph.D. thesis, University Berlin (TU), Germany, 1996.
[36] D. Helm, in: R.R. Boyer, D. Eylon, G. Lütjering (Eds.), Fatigue Behavior of Titanium Alloys, The Minerals, Metals & Materials Society, Warrendale, PA, 1999, p. 291.
[37] J. Lindemann, K. Gossmann, T. Raczek, L. Wagner, in: L. Wagner (Ed.), Proceedings of the Eighth International Conference on Shot Peening, Garmisch-Partenkirchen, Germany, 2002, in press.
[38] H. Gray, L. Wagner, G. Lütjering, in: J.T. Barnby (Ed.), Fatigue Prevention and Design, Chamelion Press, London UK, 1986, p. 363.